ELSEVIER

Thin-Walled Structures 39 (2001) 23–44

THIN-WALLED STRUCTURES

www.elsevier.com/locate/tws

Analysis of piezoelectric bimorphs and plates with segmented actuators

Senthil S. Vel, R.C. Batra *

Department of Engineering Science and Mechanics M/C 0219, Virginia Polytechnic Institute and State University, Blacksburg, VA 24061, USA

Received 19 September 2000; accepted 23 October 2000

Abstract

Elastic plates with distributed or segmented piezoelectric layers have been analyzed using the classical laminated plate theory, the first-order shear deformation theory, and the results are compared with an analytical solution. The plate theories and the analytical solution take into account both the direct and the converse piezoelectric effects, and assume generalized plane strain deformations. The transverse displacements from both theories are in reasonable agreement. The classical lamination theory gives a discontinuous longitudinal stress at the edges of the segments whereas the analytical solution predicts a continuous curve with steep gradients. Piezoelectric bimorphs with the axis of transverse isotropy inclined at an angle to the thickness direction are also studied using the three formulations. The displacements and stresses obtained from the first-order shear deformation theory are in very good agreement with the analytical solution even for thick plates. It is advantageous to use shear bimorphs since the stresses induced in them are smaller than those in extension bimorphs.

Keywords: Embedded actuators; Extension/shear actuators; Piezoelectric bimorph; Analytical solution; Plate theory solution

1. Introduction

In recent years, piezoelectric materials have been integrated with structural systems to form a class of "smart structures". The piezoelectric materials are capable of

* Corresponding author. Tel.: +1-540-231-6051 fax: +1-540-231-4574.
E-mail address: rbatra@vt.edu (R.C. Batra).

0263-8231/01/$ - see front matter
PII: S0263-8231(00)00052-5

altering the structure's response through sensing, actuation and control. By integrating surface-bonded and embedded actuators into structural systems, desired localized strains may be induced by applying the appropriate voltage to the actuators.

In order to successfully incorporate piezoelectric actuators into structures, the mechanical interaction between the actuators and the base structure must be fully understood. Mechanical models were developed by Crawley and de Luis [1], Im and Atluri [2], Crawley and Anderson [3] and others for piezoelectric patches mounted to the top and/or the bottom surfaces of a beam. Lee [4] developed a theory for laminated plates with distributed piezoelectric layers based on the classical lamination theory. Wang and Rogers [5] applied the classical lamination theory to plates with surface-bonded or embedded piezoelectric patches. A coupled, first-order shear deformation theory for multilayered piezoelectric plates was presented by Huang and Wu [6]. Jonnalagadda et al. [7] developed a theory for piezothermoelastic laminates based on the first-order shear deformation theory and neglected the direct piezo electric effect. Mitchell and Reddy's [8] coupled higher-order theory is based on an equivalent single-layer theory for the mechanical displacements and layerwise discretization of the electric potential. Vidoli and Batra [9] have derived a refined plate theory capable of predicting the change in the thickness of a piezoelectric plate. Numerous finite element studies have also been conducted (e.g. see Robbins and Reddy [10], Heyliger et al. [11], and Batra and Liang [12]).

Ray et al. [13] and Heyliger and Brooks [14] obtained exact solutions for simply supported linear elastic laminated plates with embedded and surface-bonded distributed piezoelectric actuators. Yang et al. [15] approximated piezoelectric actuators as thin films and derived analytical solutions for simply supported edges. Vel and Batra [16] have used the Eshelby–Stroh formalism to analyze the cylindrical bending of laminated plates with distributed and segmented piezoelectric actuators. The piezoelectric actuators are treated as an integral part of the structure and the three-dimensional differential equations of equilibrium, simplified to the case of generalized plane strain deformations, are exactly satisfied at every point in the body. The analytical solution is in terms of an infinite series; the continuity conditions at the interfaces between adjoining laminae and boundary conditions at the edges are satisfied in the sense of Fourier series. The formulation admits different boundary conditions at the edges and is applicable to thick and thin laminated plates. Recently, Vel and Batra [17] generalized the method to obtain three-dimensional analytical solutions for multilayered piezoelectric rectangular plates subjected to arbitrary boundary conditions.

While plate theories have been employed in the literature to obtain the displacements and stresses for elastic laminates with embedded or surface-bonded piezoelectric layers, it is not entirely clear whether the classical assumptions used for elastic laminates, like inextensibility in the thickness direction, are applicable to such hybrid laminates. Here we study the cylindrical bending of two configurations of hybrid laminates using plate theories and compare results with those obtained by using the analytical solution technique of Vel and Batra [16]. The edge conditions and the loads are such that the three components of the displacement and the electric field are functions of the two coordinates of a point—one in the longitudinal direction

and the other in the thickness direction. The first configuration is an elastic substrate with surface-bonded or embedded piezoelectric actuators. It is studied by using the displacement field of the classical laminated plate theory (CLPT). The second configuration is that of a cantilever piezoelectric bimorph; the axis of transverse isotropy in each layer may be inclined to the thickness direction. Piezoelectric bimorphs can be used for microactuation and as "fingers" of a robot gripper for moving delicate objects in high-precision operations (e.g. see Moulson and Herbert [18] and Tzou [19]). Due to the inclination of the axes of transverse isotropy, the piezoelectric bimorph is studied by using the displacement field of the first-order shear deformation theory (FSDT).

2. Formulations of the problems

2.1. Analytical solution

We use a rectangular Cartesian coordinate system, shown in Fig. 1, to describe the infinitesimal quasistatic deformations of a piezoelectric laminate occupying the region $[0,L]\times(-\infty,\infty)\times[0,H]$ in the unstressed reference configuration. Planes $x_3=h_1,\ldots, h_n,\ldots, h_{N+1}$ describe the bottom bounding surface, the horizontal interfaces between adjoining laminae, and the top bounding surface. Planes $x_1=l_1,\ldots, l_s,\ldots, l_{S+1}$ are the left bounding surface, the vertical interfaces between adjoining laminae, and the right bounding surface respectively. The vertical interfaces are introduced to accommodate the change in the thickness of the plate due to segmented layers and/or due to discrete changes in material properties in the longitudinal direction. The region $l_s<x_1<l_{s+1}$ is referred to as segment s. The total number of such segments is denoted by S. It is assumed that the electric potential

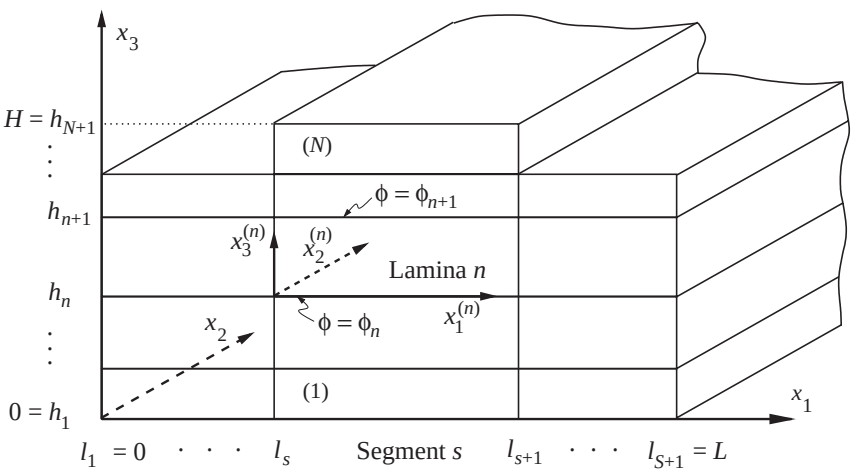

Fig. 1. Laminated plate with segmented piezoelectric actuators.

ϕ is prescribed on the top and bottom surfaces of each lamina. We postulate that the displacement and the electric potential are functions of x_1 and x_3 only and thus the laminate is in a state of generalized plane strain. This assumption is reasonable when the applied loads and material properties are independent of x_2 for a body of infinite extent in the x_2 direction. We denote the components of the mechanical displacement by u_i, the Cauchy stress tensor by σ_{ij}, the electric field by $E_i=-\partial\phi/\partial x_i$ and the electric displacement by D_i. We construct a local coordinate system $x_1^{(n)}$, $x_2^{(n)}$, $x_3^{(n)}$ for the nth lamina of segment s with origin at the point $(l_s, 0, h_n)$ in the global coordinate system and parallel to the global axes.

An analytical solution for the nth lamina of segment s that satisfies the three-dimensional equilibrium equations of piezoelectricity simplified to generalized plane strain is

$$\begin{bmatrix}\mathbf{u}\\ \phi\end{bmatrix}=\sum_{\alpha=1}^{4}[\mathbf{a}_\alpha f_\alpha(z_\alpha)+\bar{\mathbf{a}}_\alpha f_{\alpha+4}(\bar{z}_\alpha)],$$

$$\begin{bmatrix}\boldsymbol{\sigma}_1\\ D_1\end{bmatrix}=\sum_{\alpha=1}^{4}[-p_\alpha\mathbf{b}_\alpha f'_\alpha(z_\alpha)-\bar{p}_\alpha\bar{\mathbf{b}}_\alpha f'_{\alpha+4}(\bar{z}_\alpha)], \tag{1}$$

$$\begin{bmatrix}\boldsymbol{\sigma}_3\\ D_3\end{bmatrix}=\sum_{\alpha=1}^{4}[\mathbf{b}_\alpha f'_\alpha(z_\alpha)+\bar{\mathbf{b}}_\alpha f'_{\alpha+4}(\bar{z}_\alpha)],$$

where the displacement vector $\mathbf{u}=[u_1, u_2, u_3]^T$, $(\boldsymbol{\sigma}_k)_i=\sigma_{ik}$, $z_\alpha=x_1^{(n)}+p_\alpha x_3^{(n)}$ and $f'(z)=df/dz$. Here p_α, $\mathbf{a}_\alpha$, and $\mathbf{b}_\alpha$, are eigensolutions of an eigenvalue problem in the Eshelby–Stroh formulation (Vel and Batra [16]). The analytic functions $f_\alpha(\alpha=1,2,\ldots,8)$ are defined as

$$f_\alpha(z_\alpha)=\sum_{m=0}^{\infty}\{v_{m\alpha}^{(1)}\exp(\eta_{m\alpha}z_\alpha)+w_{m\alpha}^{(1)}\exp(\eta_{m\alpha}(l-z_\alpha))\}$$

$$+\sum_{k=0}^{\infty}\{v_{k\alpha}^{(3)}\exp(\lambda_{k\alpha}z_\alpha)+w_{k\alpha}^{(3)}\exp(\lambda_{k\alpha}(p_\alpha t_n-z_\alpha))\}, \tag{2}$$

$$f_{\alpha+4}(\bar{z}_\alpha)=\overline{f_\alpha(z_\alpha)},\ (\alpha=1,2,3,4),$$

where $l=l_{s+1}-l_s$, $t_n=h_{n+1}-h_n$,

$$\eta_{m\alpha}=\begin{cases}-\dfrac{m_0\pi i}{p_\alpha t_n}\ \text{if } m=0\\ -\dfrac{m\pi i}{p_\alpha t_n}\ \text{if } m\geq 1\end{cases},\quad \lambda_{k\alpha}=\begin{cases}\dfrac{k_0\pi i}{l}\ \text{if } k=0\\ \dfrac{k\pi i}{l}\ \text{if } k\geq 1\end{cases}, \tag{3}$$

$i=\sqrt{-1}$ and $m_0, k_0 \in (0,1)$

The boundary conditions at the edge $x_1^{(n)}=0$ of segment $s=1$ are specified as

$$\mathbf{J}\begin{bmatrix}\mathbf{u}\\ \phi\end{bmatrix}+\hat{\mathbf{J}}\begin{bmatrix}\boldsymbol{\sigma}_1\\ D_1\end{bmatrix}=\mathbf{f}(x_3), \tag{4}$$

where the function $\mathbf{f}(x_3)$ is prescribed and $\mathbf{J}$, $\hat{\mathbf{J}}$ are 4×4 diagonal matrices with entries either zero or one such that $\mathbf{J}+\hat{\mathbf{J}}=\mathbf{I}$, and $\boldsymbol{I}$ is the 4×4 identity matrix. For example, if the edge is clamped (C) and the normal component of the electric displacement on it is zero, then $\mathbf{J}=diag[1,1,1,0]$, $\hat{\mathbf{J}}=diag[0,0,0,1]$ and $\mathbf{f}=\mathbf{0}$. If the edge is traction-free (F) and the normal component of the electric displacement on it is zero, then $\mathbf{J}=diag[0,0,0,0]$, $\hat{\mathbf{J}}=diag[1,1,1,1]$ and $\mathbf{f}=\mathbf{0}$. Similarly, the boundary conditions may be specified on the edge $x_1^{(n)}=l_{S+1}$ and the top and bottom surfaces of the laminate. The displacements, the traction vector and the normal component of the electric displacement are assumed to be continuous at every point on the vertical interfaces between segments s and $s+1$. The displacements and the traction vector are assumed to be continuous across the horizontal interfaces between laminae n and $n+1$, and the potential is assumed to be known. We obtain the coefficients $v_{m\alpha}^{(j)}$ and $w_{m\alpha}^{(j)}$ (j=1,2) in (2) by using the classical Fourier series method to enforce the boundary conditions on the bounding surfaces and the continuity conditions at the interfaces between adjoining laminae (Vel and Batra [16]).

2.2. CLPT analysis

In this section we analyze elastic plates with segmented piezoelectric layers by using the displacement field consistent with the CLPT (for brevity, the solution is referred to as the CLPT solution). Each lamina is made of a monoclinic material with x_2=0 as the symmetry plane. We assume the following axial and transverse displacement field (e.g. see Jones [20]) for segment s of the laminate:

$$\begin{aligned} u_1(x_1,x_3)&=u_1^0(x_1)-x_3\frac{\mathrm{d}u_3^0}{\mathrm{d}x_1},\\ u_3(x_1,x_3)&=u_3^0(x_1), \end{aligned} \tag{5}$$

where $u_1{}^0(x_1)$ and $u_3{}^0(x_1)$ are the axial and the transverse displacements of a point on the reference surface x_3=0. The infinitesimal longitudinal strain associated with the displacement field is

$$\varepsilon_{11}=\frac{\mathrm{d}u_1^0}{\mathrm{d}x_1}-x_3\frac{\mathrm{d}^2u_3^0}{\mathrm{d}x_1^2}. \tag{6}$$

The other components of the strain tensor are identically zero. The constitutive relationship for a piezoelectric material with its axis of transverse isotropy in the x_3 direction is given in Appendix A. It is assumed that all layers are in a state of plane stress and the in-plane electric field components are negligible as compared to the intensity of the transverse electric field, i.e. $|E_1^{(n)}|\ll|E_3^{(n)}|$. With contributions from $E_1^{(n)}$ neglected in the constitutive relation, the reduced stress–strain relationship can be written (e.g. see Benjeddou et al. [21]) as

$$\begin{bmatrix}\sigma_{11}\\ D_3\end{bmatrix}^{(n)}=\begin{bmatrix}\bar{Q}_{11} & -\bar{e}_{31}\\ \bar{e}_{31} & \bar{\epsilon}_{33}\end{bmatrix}^{(n)}\begin{bmatrix}\varepsilon_{11}\\ E_3^{(n)}\end{bmatrix}, \tag{7}$$

where σ_{11} is the longitudinal stress, D_3 is the component of the electric displacement in the thickness direction, $E_3^{(n)}$ is the electric field in the thickness direction, and

$$\bar{Q}_{11}^{(n)}=C_{11}^{(n)}-(C_{13}^{(n)})^2/C_{33}^{(n)},\ \bar{e}_{31}^{(n)}=e_{31}^{(n)}-C_{13}^{(n)}e_{33}^{(n)}/C_{33}^{(n)},\ \bar{\epsilon}_{33}^{(n)}=\epsilon_{33}^{(n)}+(e_{33}^{(n)})^2/C_{33}^{(n)}. \tag{8}$$

Here $\bar{Q}_{11}^{(n)},\bar{e}_{31}^{(n)},\bar{\epsilon}_{33}^{(n)}$ are the reduced elastic stiffness, piezoelectric coefficient and dielectric permittivity respectively of the nth lamina.

The transverse component of the electric displacement obtained from (7) and (6) is

$$D_3^{(n)}=\bar{e}_{31}^{(n)}\left(\frac{\mathrm{d}u_1^0}{\mathrm{d}x_1}-x_3\frac{\mathrm{d}^2u_3^0}{\mathrm{d}x_1^2}\right)-\bar{\epsilon}_{33}^{(n)}\frac{\partial\phi^{(n)}}{\partial x_3}. \tag{9}$$

With the assumption that $|D_{1,1}^{(n)}|\ll|D_{3,3}^{(n)}|$, the charge equation of electrostatics reduces to

$$D_{3,3}^{(n)}=-\bar{e}_{31}^{(n)}\frac{\mathrm{d}^2u_3^0}{\mathrm{d}x_1^2}-\bar{\epsilon}_{33}^{(n)}\frac{\partial^2\phi^{(n)}}{\partial x_3^2}=0. \tag{10}$$

Integration of (10) gives the following expressions for the electric potential and the electric field in lamina n:

$$\begin{aligned}\phi^{(n)}&=\frac{\phi_{n+1}+\phi_n}{2}+\frac{\phi_{n+1}-\phi_n}{t_n}(x_3-\bar{h}_n)+\left[1-4\left(\frac{x_3-\bar{h}_n}{t_n}\right)^2\right]\frac{\bar{e}_{31}^{(n)}t_n^2}{\bar{\epsilon}_{33}^{(n)}8}\frac{\mathrm{d}^2u_3^0}{\mathrm{d}x_1^2},\\ E_3^{(n)}&=-\frac{\phi_{n+1}-\phi_n}{t_n}+\frac{\bar{e}_{31}^{(n)}}{\bar{\epsilon}_{33}^{(n)}}(x_3-\bar{h}_n)\frac{\mathrm{d}^2u_3^0}{\mathrm{d}x_1^2},\end{aligned} \tag{11}$$

where $t_n=h_{n+1}-h_n$ and $\bar{h}_n=(h_{n+1}+h_n)/2$ are the thickness and the midsurface coordinate of lamina n, respectively. The second term in the expression for the electric field E_3 in (11) is the potential induced in the nth lamina due to the deformation of the plate, i.e. the direct piezoelectric effect. Our formulation parallels that of Benjeddou et al. [21] who retained this term, although it is often neglected.

The variational principle for a piezoelectric medium (e.g. see Tiersten [22]) gives the following governing equations

$$\begin{aligned}&\frac{\mathrm{d}N_{11}}{\mathrm{d}x_1}=0,\\ &\frac{\mathrm{d}^2M_{11}}{\mathrm{d}x_1^2}+q=0,\end{aligned} \tag{12}$$

where

$$N_{11}=\sum_{n=1}^{N}\int_{h_n}^{h_{n+1}}\sigma_{11}^{(n)}\mathrm{d}x_3, \tag{13}$$

$$M_{11}=\sum_{n=1}^{N}\int_{h_n}^{h_{n+1}}[\sigma_{11}^{(n)}x_3+D_3^{(n)}\frac{\bar{e}_{31}^{(n)}}{\bar{\epsilon}_{33}^{(n)}}(x_3-\bar{h}_n)]\mathrm{d}x_3,$$

and q is the normal surface traction. Substitution for the longitudinal stress and the transverse electric displacement from (7) into (13) and the result into (12) yields the following equations in terms of the displacements of the reference surface

$$A_{11}\frac{\mathrm{d}^2u_1^0}{\mathrm{d}x_1^2}-(B_{11}+B_{11}^d)\frac{\mathrm{d}^3u_3^0}{\mathrm{d}x_1^3}-\frac{dN_{11}^c}{\mathrm{d}x_1}=0, \tag{14}$$

$$(B_{11}+B_{11}^d)\frac{\mathrm{d}^3u_1^0}{\mathrm{d}x_1^3}-(D_{11}+D_{11}^d)\frac{\mathrm{d}^4u_3^0}{\mathrm{d}x_1^4}-\frac{\mathrm{d}^2M_{11}^c}{\mathrm{d}x_1^2}+q=0.$$

The superscripts c and d respectively denote the contributions due to the converse and the direct piezoelectric effects, and

$$[A_{ij},B_{ij},D_{ij}]=\sum_{n=1}^{N}\int_{h_n}^{h_{n+1}}\bar{Q}_{ij}^{(n)}[1,x_3,x_3^2]\mathrm{d}x_3,$$

$$[B_{ij}^d,D_{ij}^d]=\sum_{n=1}^{N}\int_{h_n}^{h_{n+1}}\frac{\bar{e}_{3i}^{(n)}\bar{e}_{3j}^{(n)}}{\bar{\epsilon}_{33}^{(n)}}[x_3-\bar{h}_n,\ x_3^2-\bar{h}_n^2]\mathrm{d}x_3, \tag{15}$$

$$[N_{11}^c,M_{11}^c]=-\sum_{n=1}^{N}\int_{h_n}^{h_{n+1}}\frac{\bar{e}_{31}^{(n)}(\phi_{n+1}-\phi_n)}{t_n}[1,\bar{h}_n]\mathrm{d}x_3.$$

The variational principle also gives the following continuity conditions on the vertical interface $x_1=l_{s+1}$ between the segments s and $s+1$.

$$[\![u_1^0]\!]=0,\ [\![u_3^0]\!]=0,[\![\frac{\mathrm{d}u_3^0}{\mathrm{d}x_1}]\!]=0,\ [\![N_{11}]\!]=0,\ [\![\frac{\mathrm{d}M_{11}}{\mathrm{d}x_1}]\!]=0,\ [\![M_{11}]\!]=0, \tag{16}$$

where $[\![u_1^0]\!]$ denotes the jump in the value of $u_1{}^0$ across the vertical interface. We assume the following boundary conditions in the CLPT for clamped (C) and traction-free (F) edges at $x_1=0$ and $x_1=L$,

$$\begin{aligned}&\text{C: } u_1^0=u_3^0=0,\ \frac{\mathrm{d}u_3^0}{\mathrm{d}x_1}=0,\\ &\text{F: } N_{11}=0,\ M_{11}=0,\ \frac{\mathrm{d}M_{11}}{\mathrm{d}x_1}=0.\end{aligned} \tag{17}$$

Substituting for $\mathrm{d}^2u_1{}^0/\mathrm{d}x_1{}^2$ from $(14)_1$ into $(14)_2$ yields a fourth-order ordinary

differential equation in $u_3{}^0$. The linear ordinary differential equations (14) for all segments together with the continuity conditions (16) and boundary conditions (17) are solved analytically using Mathematica [23] to obtain the displacements $u_1^0(x_1)$ and $u_3^0(x_1)$ and hence the stress σ_{11}. Other components of the stress tensor are computed by integrating the 3-dimensional equations of electro-elastostatics.

2.3. FSDT analysis

Consider an N-layer plate with each layer made of a piezoelectric material whose axis of transverse isotropy is inclined to the vertical as shown in Fig. 2. All laminae are assumed to be of equal width and extend from $x_1=0$ to L. Let the axis of transverse isotropy **P** (poling direction) of lamina n be inclined at an angle α_n, to the x_3-axis. The material properties of a lamina whose axis of transverse isotropy is inclined to the vertical are obtained by a coordinate transformation of its properties when its axis of transverse isotropy is in the thickness direction (see Appendix A). Since the shear strains may be non-zero due to the piezoelectric coefficients e_{15}, e_{24}, e_{26} and e_{35} in the constitutive equation, we assume the following displacement field based on the FSDT,

$$\begin{aligned} u_1(x_1,x_3)&=u_1^0(x_1)+x_3\varphi_1(x_1),\\ u_3(x_1,x_3)&=u_3^0(x_1), \end{aligned} \tag{18}$$

where $u_1^0(x_1)$ and $u_3^0(x_1)$ are the axial and the transverse displacements of a point on the bottom surface and $\varphi_1(x_1)$ is the rotation of the normal about the x_2-axis. The non-zero components of the infinitesimal longitudinal strain ε_{11} and shear strain ε_{13} associated with the displacement field (18) are

$$\varepsilon_{11}=\frac{\mathrm{d}u_1^0}{\mathrm{d}x_1}+x_3\frac{\mathrm{d}\varphi_1}{\mathrm{d}x_1},\ 2\varepsilon_{13}=\frac{\mathrm{d}u_3^0}{\mathrm{d}x_1}+\varphi_1. \tag{19}$$

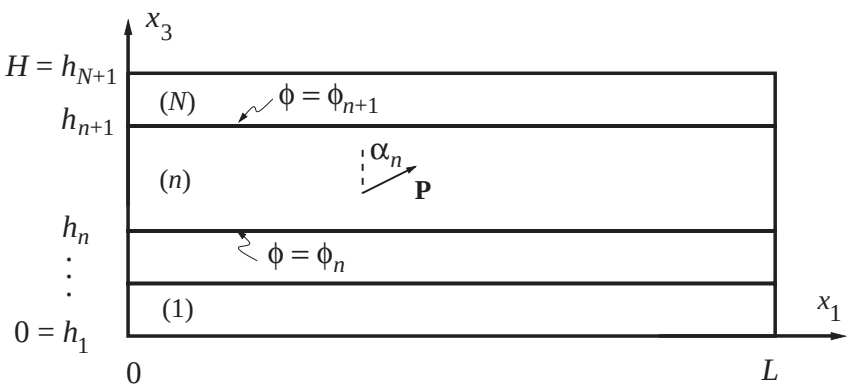

Fig. 2. N-layer piezoelectric laminate with axis of transverse isotropy inclined to the x_3-axis.

A state of plane stress is assumed in all the layers. The reduced stress–strain relation may be written as

$$\begin{bmatrix}\sigma_{11}\\ \sigma_{13}\\ D_3\end{bmatrix}^{(n)}=\begin{bmatrix}\bar{Q}_{11} & \bar{Q}_{15} & -\bar{e}_{31}\\ \bar{Q}_{15} & \bar{Q}_{55} & -\bar{e}_{35}\\ \bar{e}_{31} & \bar{e}_{35} & \bar{\epsilon}_{33}\end{bmatrix}^{(n)}\begin{bmatrix}\varepsilon_{11}\\ 2\varepsilon_{13}\\ E_3^{(n)}\end{bmatrix}, \tag{20}$$

where $\bar{Q}_{11}^{(n)},\bar{e}_{31}^{(n)},\bar{\epsilon}_{33}^{(n)}$ are the reduced material properties defined in the CLPT formulation and

$$\bar{Q}_{15}^{(n)}=C_{15}^{(n)}-C_{13}^{(n)}C_{35}^{(n)}/C_{33}^{(n)},\ \bar{Q}_{55}^{(n)}=C_{55}^{(n)}-(C_{35}^{(n)})^2/C_{33}^{(n)},\ \bar{e}_{35}^{(n)}=e_{35}^{(n)}-C_{35}^{(n)}e_{33}^{(n)}/C_{33}^{(n)}. \tag{21}$$

As stated in the previous section, we postulate that $|E_1^{(n)}|\ll|E_3^{(n)}|$ and $|D_{1,1}^{(n)}|\ll|D_{3,3}^{(n)}|$. The first of these postulates and the assumption that $E_2=0$ eliminate the effects of piezoelectric coefficients e_{15}, e_{24} and e_{26}. The transverse component of the electric displacement obtained from (20) and (19) is

$$D_3^{(n)}=\bar{e}_{31}^{(n)}\left(\frac{\mathrm{d}u_1^0}{\mathrm{d}x_1}+x_3\frac{\mathrm{d}\varphi_1}{\mathrm{d}x_1}\right)+\bar{e}_{35}^{(n)}\left(\frac{\mathrm{d}u_3^0}{\mathrm{d}x_1}+\varphi_1\right)-\bar{\epsilon}_{33}^{(n)}\frac{\partial\phi^{(n)}}{\partial x_3}. \tag{22}$$

The charge equation of electrostatics reduces to

$$D_{3,3}^{(n)}=\bar{e}_{31}^{(n)}\frac{\mathrm{d}\varphi_1}{\mathrm{d}x_1}-\bar{\epsilon}_{33}^{(n)}\frac{\partial^2\phi^{(n)}}{\partial x_3^2}=0. \tag{23}$$

Integrating this equation leads to the following expressions for the electric potential and the electric field in the nth lamina:

$$\phi^{(n)}=\frac{\phi_{n+1}+\phi_n}{2}+\frac{\phi_{n+1}-\phi_n}{t_n}(x_3-\bar{h}_n)-[1-4(\frac{x_3-\bar{h}_n}{t_n})^2]\frac{\bar{e}_{31}^{(n)}t_n^2}{\bar{\epsilon}_{33}^{(n)}8}\frac{\mathrm{d}\phi_1}{\mathrm{d}x_1}, \tag{24}$$

$$E_3^{(n)}=-\frac{\phi_{n+1}-\phi_n}{t_n}-\frac{\bar{e}_{31}^{(n)}}{\bar{\epsilon}_{33}^{(n)}}(x_3-\bar{h}_n)\frac{\mathrm{d}\phi_1}{\mathrm{d}x_1}.$$

The variational principle for a piezoelectric medium gives the following governing equations

$$\frac{dN_{11}}{dx_1}=0,$$
$$\frac{dQ_1}{dx_1}+q=0,$$
$$\frac{dM_{11}}{dx_1}-Q_1=0, \tag{25}$$

where q is the normal surface traction, N_{11} and M_{11} are given by (13) and

$$Q_1=\sum_{n=1}^{N}\int_{h_n}^{h_{n+1}}\kappa\sigma_{13}^{(n)}dx_3. \tag{26}$$

Here κ is the shear correction coefficient. We set κ=5/6 for a laminated plate even though this value was proposed for a homogeneous isotropic plate by Reissner [24]. Substitution of (20) into (13) and (26) and the result into (25) yields the following equations for the displacements of the bottom surface and rotation of the normal:

$$\begin{aligned}
&A_{11}\frac{d^2u_1^0}{dx_1^2}+(B_{11}+B_{11}^d)\frac{d^2\varphi_1}{dx_1^2}+A_{15}\left(\frac{d^2u_3^0}{dx_1^2}+\frac{d\varphi_1}{dx_1}\right)-\frac{dN_{11}^c}{dx_1}=0,\\
&\kappa A_{15}\frac{d^2u_1^0}{dx_1^2}+\kappa(B_{15}+B_{15}^d)\frac{d^2\varphi_1}{dx_1^2}+\kappa A_{55}\left(\frac{d^2u_3^0}{dx_1^2}+\frac{d\varphi_1}{dx_1}\right)-\kappa\frac{dQ_1^c}{dx_1}+q=0,\\
&(B_{11}+B_{11}^d)\frac{d^2u_1^0}{dx_1^2}+(D_{11}+D_{11}^d)\frac{d^2\varphi_1^0}{dx_1^2}+(B_{15}+B_{15}^d)\left(\frac{d^2u_3^0}{dx_1^2}+\frac{d\varphi_1}{dx_1}\right)-\frac{dM_{11}^c}{dx_1}\\
&-\kappa A_{15}\frac{du_1^0}{dx_1}-\kappa(B_{15}+B_{15}^d)\frac{d\varphi_1}{dx_1}-\kappa A_{55}\left(\frac{du_3^0}{dx_1}+\varphi_1\right)+\kappa Q_1^c=0,
\end{aligned} \tag{27}$$

where the A's, B's, D's, N_{11}^c and M_{11}^c are defined in (15) and

$$Q_1^c=-\sum_{n=1}^{N}\int_{h_n}^{h_{n+1}}\bar{e}_{35}^{(n)}\frac{(\phi_{n+1}-\phi_n)}{t_n}dx_3. \tag{28}$$

We assume the following boundary conditions in the FSDT for clamped (C) and traction-free (F) edges at x_1=0 and L,

$$\begin{aligned}
&\text{C: } u_1^0=u_3^0=0,\varphi_1=0,\\
&\text{F: } N_{11}=0,M_{11}=0,Q_1=0.
\end{aligned} \tag{29}$$

The linear ordinary differential equations (27) with the associated boundary con-

ditions (29) are solved analytically using Mathematica [23] for the displacements u_1^0, u_3^0 and rotation φ_1. Stress component $\sigma_{11}^{(n)}$ is computed using Eq. (20), and the remaining components of the stress tensor are evaluated by integrating the equilibrium equations.

3. Results and discussion

3.1. Elastic substrate with segmented actuators

We consider a homogeneous graphite-epoxy cantilever substrate with segmented PZT-5A actuators bonded to its upper and lower surfaces as shown in Fig. 3(a). This particular problem was studied by Crawley and Anderson [3] by using the Euler–Bernoulli beam model. If the surfaces x_3=0 and H are subjected to an identical elec-

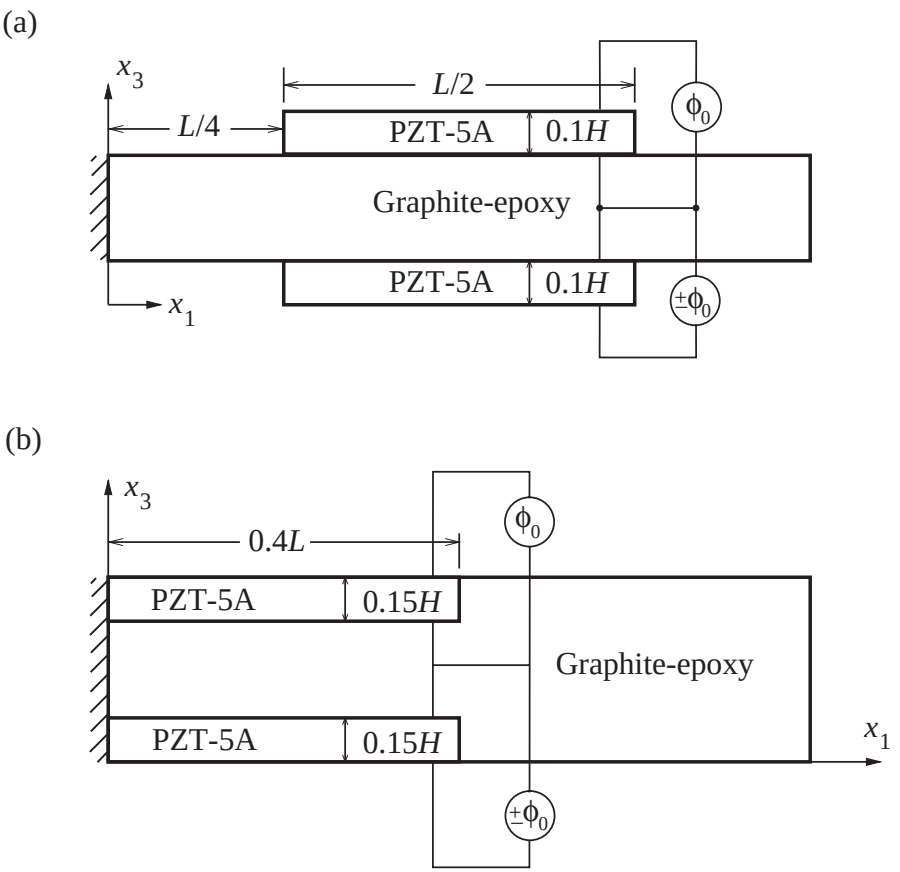

Fig. 3. Elastic substrate with (a) surface-bonded piezoelectric actuators and (b) embedded piezoelectric actuators.

tric potential ϕ_0, one of the actuators will elongate in the longitudinal direction and the other will contract, causing the plate to bend. If opposite electric potentials $-\phi_0$ and ϕ_0 are applied to the surfaces x_3=0 and H respectively, both layers will either elongate or contract, thus causing axial extension or contraction of the plate. In order to accommodate the abrupt change in the thickness of the plate due to the segmented piezoelectric actuators, the span is divided into three segments by introducing virtual vertical interfaces at x_1=L/4 and 3L/4. The continuity conditions (16) are enforced across the vertical interfaces between the segments. The second configuration, depicted in Fig. 3(b), has piezoelectric actuators embedded into the graphite-epoxy substrate. We introduce a vertical interface at x_1=0.4L due to the abrupt change in material properties across this surface. The span-to-thickness ratio (L/H) for the plate with surface-bonded actuators is 10, while the plate with embedded actuators is thicker with L/H=5. The non-zero material properties of the graphite-epoxy and the PZT-5A (poled in the x_3-direction), taken from Tang et al. [25], are listed in Table 1.

The following non-dimensionalization of the displacements and stresses is used:

$$\tilde{u}_k=\frac{C_0 u_k}{e_0\varphi_0},\ \tilde{\sigma}_{jk}=\frac{L\sigma_{jk}}{e_0\varphi_0},$$

where C_0=99.201 GPa and e_0=−7.209 cm^{-2}. The transverse deflection in bending, and the axial deformation in elongation are depicted in Fig. 4(a,b) respectively for the plate with surface-bonded actuators. The CLPT overestimates the tip deflection by 10% in bending mode and by 13% in elongation mode as compared to the analytical solution. The corresponding results for the plate with embedded actuators are given in Fig. 4(c,d). The differences in the tip deflection for this case are 4 and 6%

Table 1
Non-vanishing material properties of graphite-epoxy and PZT-5A

Material property	Graphite epoxy	PZT-5A
C_{11} (GPa)	183.443	99.201
C_{22} (Gpa)	11.662	99.201
C_{33} (GPa)	11.662	86.856
C_{12} (GPa)	4.363	54.016
C_{13} (GPa)	4.363	50.778
C_{23} (GPa)	3.918	50.778
C_{44} (GPa)	2.870	21.100
C_{55} (GPa)	7.170	21.100
C_{66} (GPa)	7.170	22.593
e_{31} (cm^{-2})	0	−7.209
e_{32} (cm^{-2})	0	−7.209
e_{33} (cm^{-2})	0	15.118
e_{24} (cm^{-2})	0	12.322
e_{15} (cm^{-2})	0	12.322
ϵ_{11} (10^{-8} F/m)	1.53	1.53
ϵ_{22} (10^{-8} F/m)	1.53	1.53
ϵ_{33} (10^{-8} F/m)	1.53	1.50

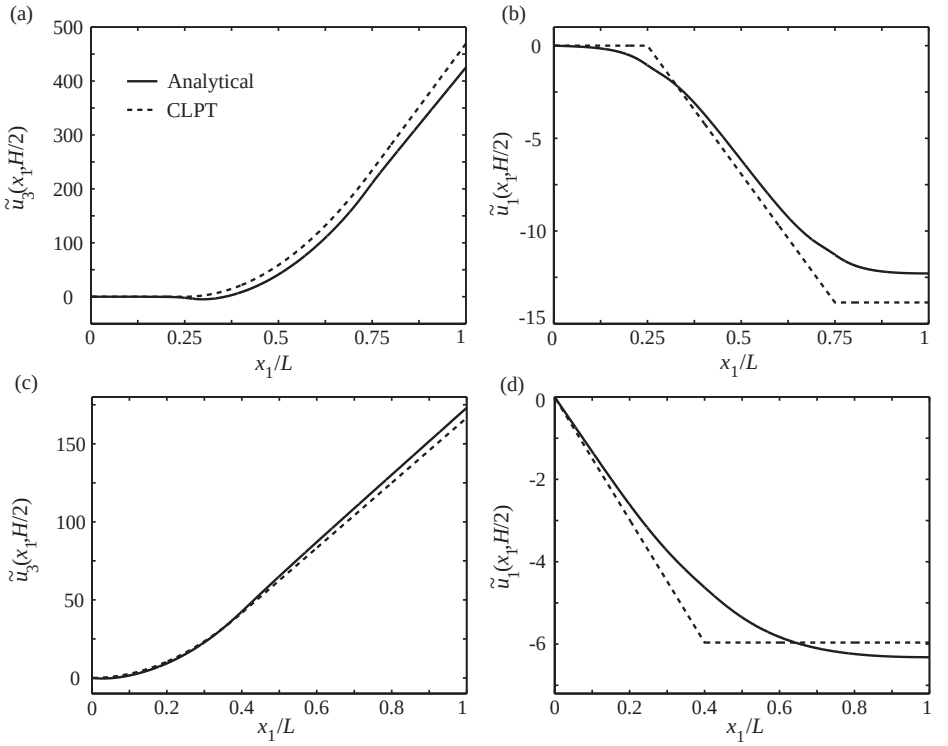

Fig. 4. Longitudinal distribution of (a) transverse displacement in bending and (b) axial displacement in extension for surface-bonded actuators; (c) transverse displacement in bending and (d) axial displacement in extension for embedded actuators.

in bending and elongation modes respectively. The deviations are smaller for the plate with embedded actuators although it is thicker than the plate with surface-mounted actuators. The CLPT predicts a linear variation in the longitudinal direction of the axial displacement in the segment with piezoelectric actuators [see Fig. 4(b and d)] and a constant value in the other segment(s). In comparison the analytical solution gives a smooth variation of the axial displacement. An explanation is that the CLPT is designed to account for the bending of the plate due to normal tractions applied on its upper and lower surfaces. Equation $(15)_3$ implies that N^c_{11} and M^c_{11} vanish in the portions of the plate without the PZTs. In the absence of axial forces these parts of the substrate undergo rigid motions.

The axial variation of the longitudinal stress in the graphite-epoxy substrate is depicted in Fig. 5(a) for the bending mode and in Fig. 5(b) for the extension mode for the plate with surface-bonded actuators. The corresponding results for embedded actuators are plotted in Fig. 5(c,d). The CLPT predicts a piecewise constant longitudinal stress along the span of the plate. The discontinuity at the vertical interfaces between the segments is because the continuity of the longitudinal stress is satisfied only in an average sense. In comparison we obtain a continuous longitudinal stress

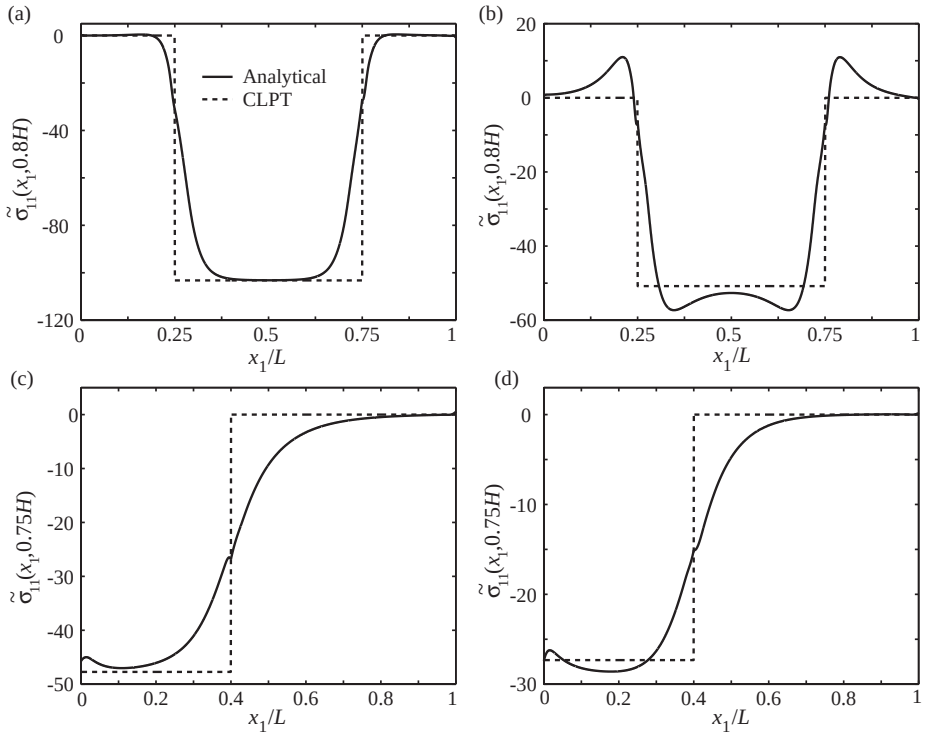

Fig. 5. Longitudinal distribution of the axial stress in the substrate for (a) bending and (b) extension with surface-bonded actuators; (c) bending and (d) extension with embedded actuators.

from the analytical solution since the continuity of the traction is enforced at every point along the vertical interfaces between the segments. The kinks in the analytical solution for the longitudinal stress across the vertical interface between adjacent segments are due to the truncation of the infinite series in (2) to 800 terms. The consideration of more terms reduces and even eliminates these kinks. The through-thickness distribution of the longitudinal stress at two locations within the piezoelectric actuators is plotted in Fig. 6. Fig. 6(a) corresponds to the bending and Fig. 6(b) is for the extension of the plate with surface-bonded actuators. The CLPT gives a piecewise linear variation of the longitudinal stress in the bending mode and a piecewise constant variation in the extension mode. The analytical and the CLPT curves almost overlap at the midsection $x_1=0.5L$, but there is significant deviation near the edge of the piezoelectric segment at $x_1=0.7L$. The corresponding through-thickness variations of the longitudinal stress for embedded actuators are shown in Fig. 6(c,d). Their behavior is qualitatively similar to that observed in plates with surface-mounted actuators.

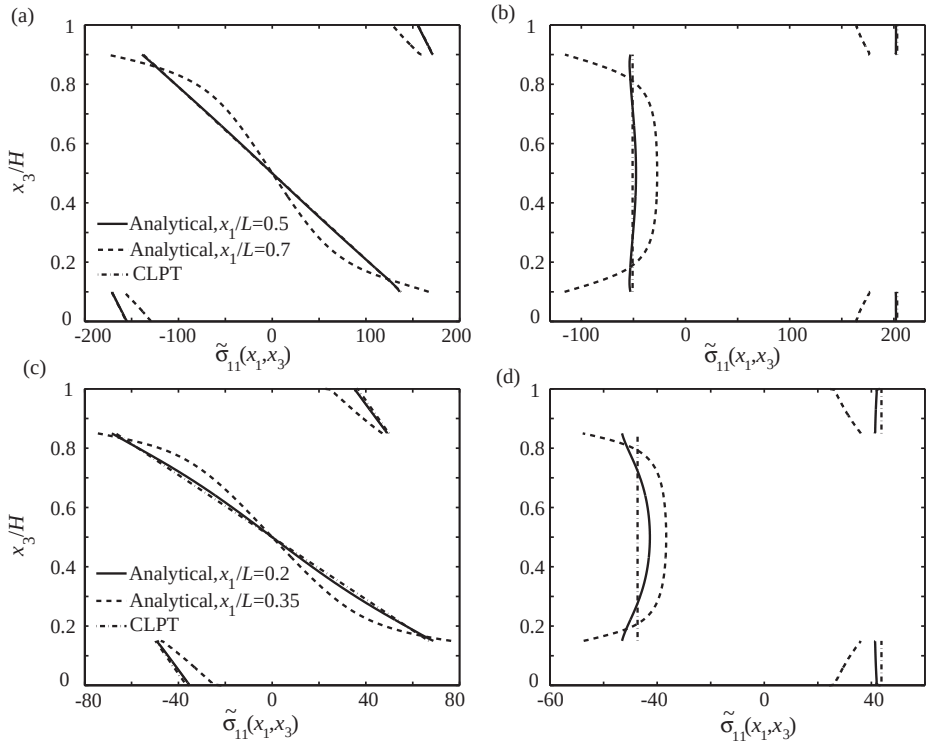

Fig. 6. Through-thickness distribution of the axial stress in the actuators and substrate for (a) bending and (b) extension with surface-bonded actuators; (c) bending and (d) extension with embedded actuators.

3.2. Extension-shear bimorph

Consider a cantilever bimorph made of two transversely isotropic piezoelectric layers of equal thickness with the axis of transverse isotropy inclined to the normal to the plate as shown in Fig. 7. When α=0, the direction of transverse isotropy in the two layers points in opposite directions. The piezoelectric coefficient e_{31} for the two layers is of equal magnitude but of opposite signs since $e_{31}(0°)=e_{31}$ and

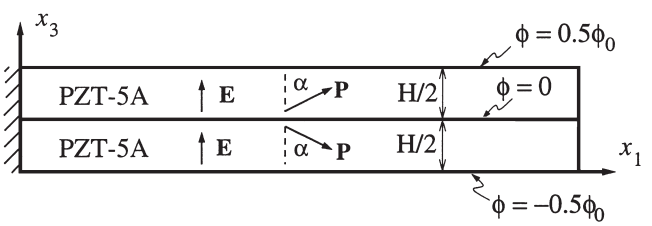

Fig. 7. Cantilever piezoelectric bimorph configuration.

$e_{31}(180°)=-e_{31}$. Thus the application of an electric field causes one layer to elongate in the axial direction and the other to contract, forcing the piezoelectric bimorph to bend in the transverse direction. This is referred to as an *extension bimorph*. It is the conventional bimorph configuration found in the literature (Moulson and Herbert [18] and Tzou [19]). When $\alpha=90°$, the polarizations in both layers are parallel to the x_1-axis and $e_{35}(90°)=e_{15}$,$e_{26}(90°)=e_{24}$. Since $E_2=0$ for the cylindrical bending problem, therefore e_{24} does not induce any shear deformations. The application of an electric field in the x_3-direction would produce a pure shear deformation of the bimorph thus causing it to deflect in the transverse direction. This configuration is known as a *shear bimorph*. Zhang and Sun [26] have studied sandwich structures with cores made of shear mode piezoelectric materials. For intermediate values of α ($0°<\alpha<90°$), both $e_{31}(\alpha)$ and $e_{35}(\alpha)$ are in general non-zero for both layers and the transverse deflection is due to a combination of extension as well as shear deformation even when an electric field is applied only in the x_3-direction. We refer to such a configuration as a *combined extension-shear bimorph*. Vidoli and Batra [9] have used their refined plate theory to study deformations of a single layer of piezoelectric material with the axis of transverse isotropy inclined at an angle to the vertical axis.

The variation of the transverse tip deflection with α is depicted in Fig. 8(a,b) for length-to-thickness ratios of 10 and 5 respectively. The FSDT solution compares very well with the analytical solution for all values of α, and the CLPT results are good only for small values of α. This is because the coefficient e_{35} does not appear in the CLPT formulation and it cannot account for shear deformation. The analytical and the FSDT solutions show that the maximum tip deflection is realized in a combined extension-shear bimorph at $\alpha\simeq20°$ when the span-to-thickness ratio is 10 and at $\alpha\simeq28°$ when the ratio is 5. In general, this angle would depend on the material properties of the laminae. Fig. 8(c,d) depict the variation of the longitudinal stress at the midspan versus α. The CLPT and the FSDT capture the behavior of the longitudinal stress very well for all values of α. It should be noted that, for a given tip deflection, the longitudinal stress is significantly smaller in a shear bimorph than that in an extension bimorph.

The transverse deflection of the midsurface of the bimorph with $L/H=5$ is plotted in Fig. 9 for angles $\alpha=0°$, 30°, 60° and 90°. It is parabolic for an extension bimorph and linear for a shear actuation bimorph as shown in Fig. 9(a and d). The FSDT gives very accurate transverse deflection at all points along the span, for all angles. As expected, the CLPT results are in significant error for large values of α. Fig. 10 depicts the through-thickness distribution of the electric field, the axial displacement, the transverse deflection and the longitudinal stress for $\alpha=45°$ and $L/H=5$. The analytical solution for the electric field at the midspan shown in Fig. 10(a) has a piecewise linear variation within each layer except at points close to the top and bottom surfaces. The electric field has been nondimensionalized as $\tilde{E}_3=-E_3H/\varphi_0$. The CLPT and the FSDT are able to capture this linear behavior since the formulation accounts for the direct piezoelectric effect. The through-thickness variation of the axial tip deflection predicted by all three theories is essentially the same [Fig. 10(b)]. The analytical solution predicts that the top and bottom surfaces of the bimorph deflect

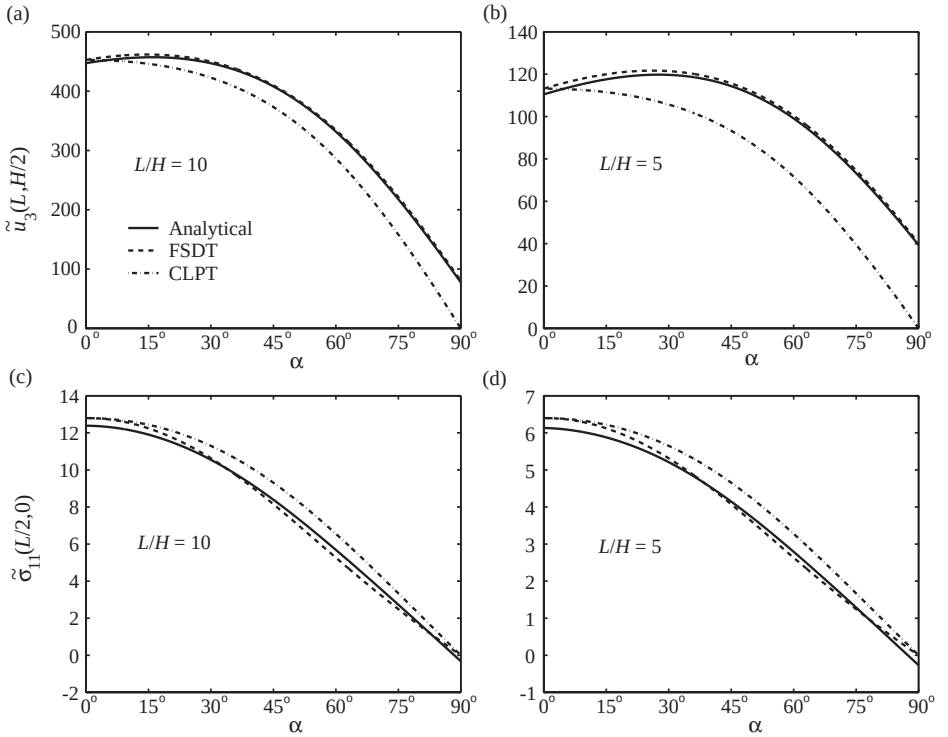

Fig. 8. Tip deflection of a bimorph versus angle α for two span-to-thickness ratios (a, b) and midplane longitudinal stress versus angle α for two span-to-thickness ratios (c, d).

more than the midsurface as shown in Fig. 10(c). Thus the thickness of the upper layer increases and that of the lower one decreases. The FSDT assumes a constant transverse deflection through the thickness of the bimorph, and is able to capture the average transverse deflection. The through-thickness variation of the longitudinal stress near the free edge of the bimorph is depicted in Fig. 10(d). The analytical solution deviates noticeably from the piecewise linear distribution of the CLPT and the FSDT. The through-thickness distribution of σ_{13} obtained from the analytical solution at a location close to the free edge is plotted in Fig. 11 for various values of the angle α. The FSDT results are not shown since it cannot capture the highly localized behavior of the transverse shear stress. The shear stress is largest on the interface between the bimorphs and decreases as α increases. It is negligible for shear bimorphs (α=90°). Thus, for a given tip deflection, the transverse shear stress on the interface and the longitudinal stress are significantly smaller for shear bimorphs than those for extension bimorphs.

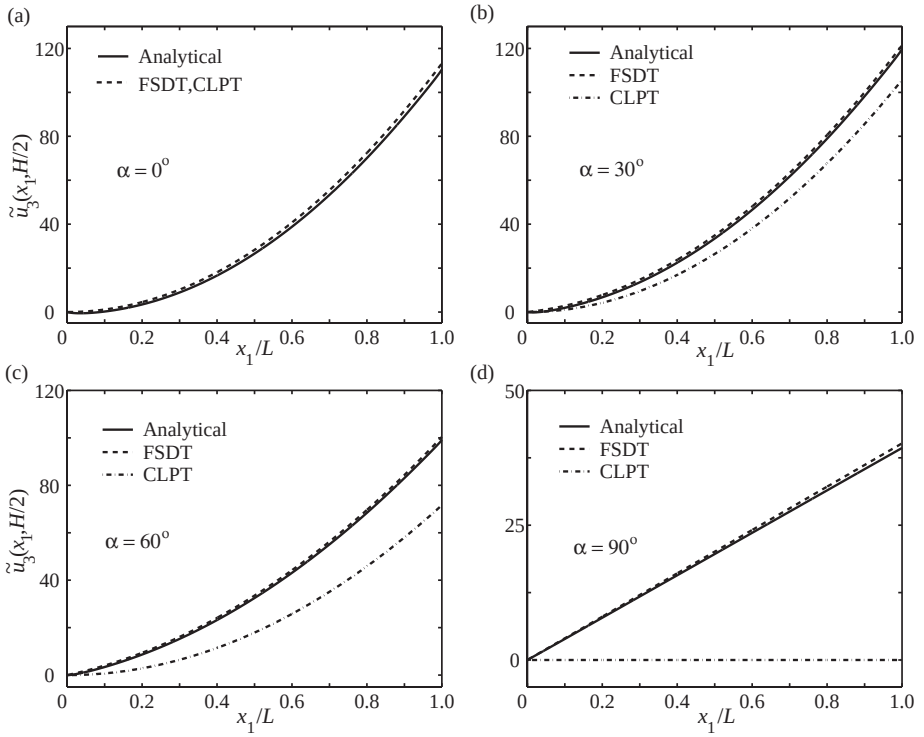

Fig. 9. Longitudinal distribution of transverse deflection for a bimorph: (a)α=0°, (b)α=30°, (a)α=60°, (a)α=90°. L/H=5.

4. Conclusions

Elastic plates with distributed or segmented piezoelectric layers have been analyzed by using three different formulations. The first is an analytical technique wherein the three-dimensional equilibrium equations of piezoelectricity are satisfied exactly, and the boundary conditions on the bounding surfaces and continuity conditions on the interfaces between adjoining laminae are satisfied in the sense of Fourier series. The second formulation is based on the displacement field of the CLPT and accounts for both the direct and the converse piezoelectric effects. The third formulation, based on the displacement field of the FSDT, can be used even when the axis of transverse isotropy of the piezoelectric lamina are inclined at an angle to the thickness direction.

We have analyzed elastic plates with surface-bonded and embedded segmented actuators by using the analytical technique and the CLPT. The transverse displacements from both theories are in reasonable agreement with each other. The longitudinal stress from the CLPT is discontinuous between the segments, while that obtained from the analytical solution is continuous and has a steep gradient. We have also

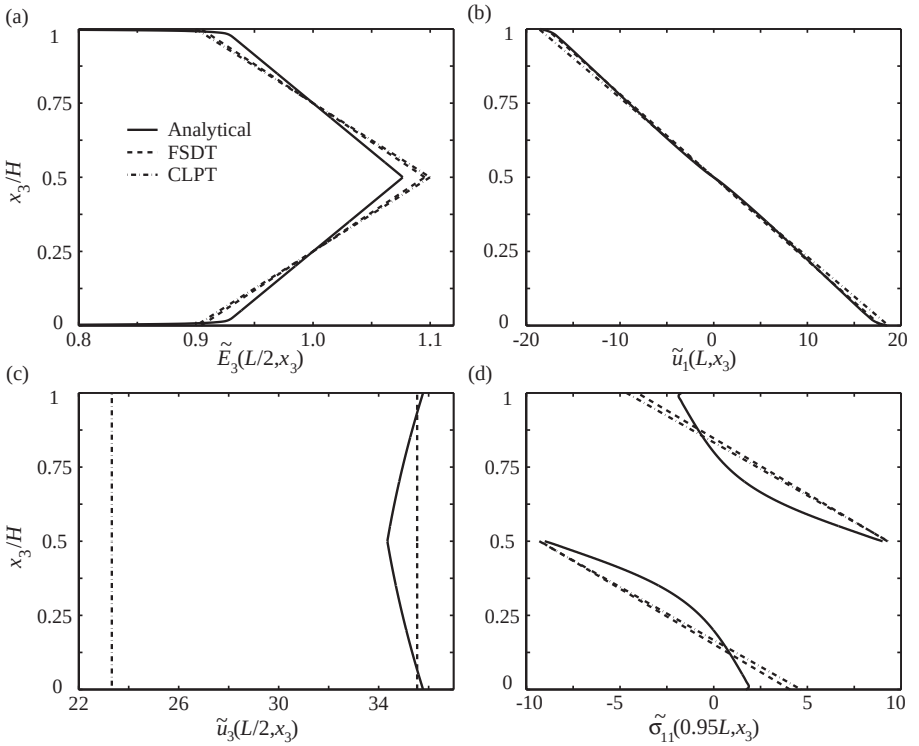

Fig. 10. Through-thickness distribution for a bimorph, α=45° and L/H=5: (a) transverse electric field, (b) axial deflection of the free edge, (c) transverse deflection at midspan and (d) longitudinal stress near free edge.

studied piezoelectric bimorphs whose axis of transverse isotropy is inclined at an angle to the thickness direction. The results for the displacements and longitudinal stress from the FSDT compare very well with those obtained from the analytical solution even for thick plates and for all angles of inclination. For the same deflection, the transverse shear stress on the interface and the longitudinal stress in shear bimorphs are substantially smaller than those in extension bimorphs. It is advantageous to use a shear bimorph since the high stresses in an extension bimorph can be detrimental to its structural integrity.

As has been shown by Vel and Batra [16] amongst others, the CLPT, the FSDT and the analytical technique used here give very good results for thin plates. The analytical method is valid for both thick and thin laminates, even when edges of adjoining laminae are subjected to different boundary conditions.

Acknowledgements

This work was partially supported by the NSF grant CMS9713453 and the ARO grant DAAG55-98-1-0030 to Virginia Polytechnic Institute and State University. R.C. Batra was also supported by an Alexander von Humboldt Award.

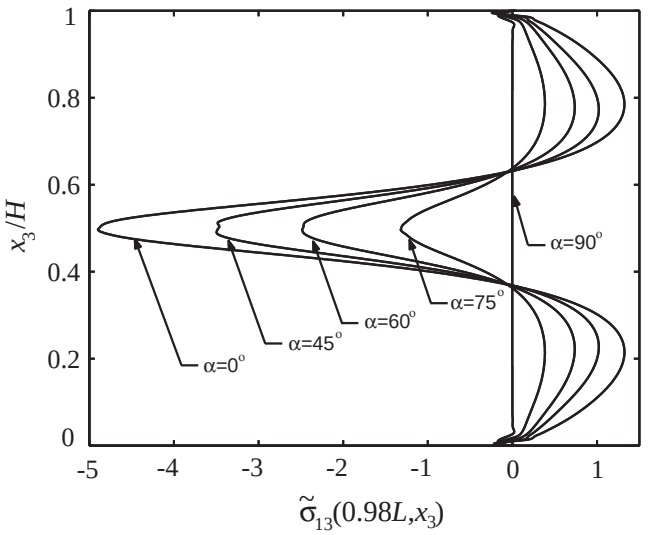

Fig. 11. Through-thickness distribution of the transverse shear stress near the free edge of a piezoelectric bimorph for five angles. L/H=5.

Appendix A

The constitutive equation for a piezoelectric material with the axis of transverse isotropy in the x_3 direction is:

$$\begin{bmatrix} \sigma_{11} \\ \sigma_{22} \\ \sigma_{33} \\ \sigma_{23} \\ \sigma_{13} \\ \sigma_{12} \\ D_1 \\ D_2 \\ D_3 \end{bmatrix} = \begin{bmatrix} C_{11} & C_{12} & C_{13} & 0 & 0 & 0 & 0 & 0 & -e_{31} \\ C_{12} & C_{22} & C_{23} & 0 & 0 & 0 & 0 & 0 & -e_{32} \\ C_{13} & C_{23} & C_{33} & 0 & 0 & 0 & 0 & 0 & -e_{33} \\ 0 & 0 & 0 & C_{44} & 0 & 0 & 0 & -e_{24} & 0 \\ 0 & 0 & 0 & 0 & C_{55} & 0 & -e_{15} & 0 & 0 \\ 0 & 0 & 0 & 0 & 0 & C_{66} & 0 & 0 & 0 \\ 0 & 0 & 0 & 0 & e_{15} & 0 & \epsilon_1 & 0 & 0 \\ 0 & 0 & 0 & e_{24} & 0 & 0 & 0 & \epsilon_2 & 0 \\ e_{31} & e_{32} & e_{33} & 0 & 0 & 0 & 0 & 0 & \epsilon_3 \end{bmatrix} \begin{bmatrix} \varepsilon_{11} \\ \varepsilon_{22} \\ \varepsilon_{33} \\ 2\varepsilon_{23} \\ 2\varepsilon_{13} \\ 2\varepsilon_{12} \\ E_1 \\ E_2 \\ E_3 \end{bmatrix}$$

If the axis of transverse isotropy is inclined at an angle α to the x_3-axis (see Fig. 2), then the constitutive equation is

$$\begin{bmatrix}\sigma_{11}\\ \sigma_{22}\\ \sigma_{33}\\ \sigma_{23}\\ \sigma_{13}\\ \sigma_{12}\\ D_1\\ D_2\\ D_3\end{bmatrix}=\begin{bmatrix}C_{11}(\alpha) & C_{12}(\alpha) & C_{13}(\alpha) & 0 & C_{15}(\alpha) & 0 & -e_{11}(\alpha) & 0 & -e_{31}(\alpha)\\ C_{12}(\alpha) & C_{22}(\alpha) & C_{23}(\alpha) & 0 & C_{25}(\alpha) & 0 & -e_{12}(\alpha) & 0 & -e_{32}(\alpha)\\ C_{13}(\alpha) & C_{23}(\alpha) & C_{33}(\alpha) & 0 & C_{35}(\alpha) & 0 & -e_{13}(\alpha) & 0 & -e_{33}(\alpha)\\ 0 & 0 & 0 & C_{44}(\alpha) & 0 & C_{46}(\alpha) & 0 & -e_{24}(\alpha) & 0\\ C_{15}(\alpha) & C_{25}(\alpha) & C_{35}(\alpha) & 0 & C_{55}(\alpha) & 0 & -e_{15}(\alpha) & 0 & -e_{35}(\alpha)\\ 0 & 0 & 0 & C_{46}(\alpha) & 0 & C_{66}(\alpha) & 0 & -e_{26}(\alpha) & 0\\ e_{11}(\alpha) & e_{12}(\alpha) & e_{13}(\alpha) & 0 & e_{15}(\alpha) & 0 & \epsilon_{11}(\alpha) & 0 & \epsilon_{13}(\alpha)\\ 0 & 0 & 0 & e_{24}(\alpha) & 0 & e_{26}(\alpha) & 0 & \epsilon_{22}(\alpha) & 0\\ e_{31}(\alpha) & e_{32}(\alpha) & e_{33}(\alpha) & 0 & e_{35}(\alpha) & 0 & \epsilon_{13}(\alpha) & 0 & \epsilon_{33}(\alpha)\end{bmatrix}\begin{bmatrix}\varepsilon_{11}\\ \varepsilon_{22}\\ \varepsilon_{33}\\ 2\varepsilon_{23}\\ 2\varepsilon_{13}\\ 2\varepsilon_{12}\\ E_1\\ E_2\\ E_3\end{bmatrix}$$

where the transformed material properties are

$$C_{11}(\alpha)=C_{11}c^4+2(C_{13}+2C_{55})c^2s^2+C_{33}s^4, \qquad C_{12}(\alpha)=C_{12}c^2+C_{23}s^2,$$
$$C_{13}(\alpha)=C_{13}c^4+(C_{11}+C_{33}-4C_{55})c^2s^2+C_{13}s^4, \qquad C_{22}(\alpha)=C_{22},$$
$$C_{33}(\alpha)=C_{33}c^4+2(C_{13}+2C_{55})c^2s^2+C_{11}s^4 \qquad C_{23}(\alpha)=C_{23}c^2+C_{12}s^2$$
$$C_{15}(\alpha)=(C_{13}-C_{11}+2C_{55})c^3s+(C_{33}-C_{13}-2C_{55})cs^3, \quad C_{25}(\alpha)=(C_{23}-C_{12})cs,$$
$$C_{35}(\alpha)=(C_{33}-C_{13}-2C_{55})c^3s+(C_{13}-C_{11}+2C_{55})cs^3, \quad C_{44}(\alpha)=C_{44}c^2+C_{66}s^2,$$
$$C_{55}(\alpha)=C_{55}c^4+(C_{11}-2C_{13}+C_{33}-2C_{55})c^2s^2+C_{55}s^4, \quad C_{46}(\alpha)=(C_{44}-C_{66})cs,$$
$$C_{66}(\alpha)=C_{66}c^2+C_{44}s^2,$$
$$e_{11}(\alpha)=(e_{31}+2e_{15})c^2s+e_{33}s^3, \quad e_{12}(\alpha)=e_{32}s,$$
$$e_{13}(\alpha)=(e_{33}-2e_{15})c^2s+e_{31}s^3, \quad e_{15}(\alpha)=e_{15}c^3+(e_{33}-e_{31}-e_{15})cs^2,$$
$$e_{24}(\alpha)=e_{24}c, \qquad e_{26}(\alpha)=e_{24}s,$$
$$e_{31}(\alpha)=e_{31}c^3+(e_{33}-2e_{15})cs^2, \quad e_{32}(\alpha)=e_{32}c,$$
$$e_{33}(\alpha)=e_{33}c^3+(e_{31}+2e_{15})cs^2, \quad e_{35}(\alpha)=(e_{33}-e_{31}-e_{15})c^2s+e_{15}s^3,$$
$$\epsilon_{11}(\alpha)=\epsilon_{11}c^2+\epsilon_{33}s^2, \quad \epsilon_{22}(\alpha)=\epsilon_{22},$$
$$\epsilon_{33}(\alpha)=\epsilon_{11}s^2+\epsilon_{33}c^2, \quad \epsilon_{13}(\alpha)=cs(\epsilon_{33}-\epsilon_{11}).$$

Here $c=\cos\alpha$ and $s=\sin\alpha$.

References

[1] Crawley EF, De Luis J. Use of piezoelectric actuators as elements of intelligent structures. AIAA J 1987;25:1373–85.

[2] Im S, Atluri SN. Effects of a piezo-actuator on a finitely deformed beam subjected to general loading. AIAA J 1989;27:1801–7.

[3] Crawley EF, Anderson EH. Detailed models of piezoceramic actuation of beams. J Intell Mater Sys Struct 1990;1:4–25.

[4] Lee CK. Theory of laminated piezoelectric plates for the design of distributed sensors/actuators. Part 1: governing equations and reciprocal relationships. J Acoust Soc Am 1990;87:1144–58.
[5] Wang BT, Rogers CA. Laminate plate theory for spatially distributed induced strain actuators. J Comp Mater 1991;25:433–52.
[6] Huang JH, Wu TL. Analysis of hybrid multilayered piezoelectric plates. Int J Engng Sci 1996;34(2):171–81.
[7] Jonnalagadda KD, Blandford GE, Tauchert TR. Piezothermoelastic composite plate analysis using first-order shear-deformation theory. Comput Struct 1994;51:79–89.
[8] Mitchell JA, Reddy JN. A refined hybrid plate theory for composite laminates with piezoelectric laminae. Int J Solids Struct 1995;32(16):2345–67.
[9] Vidoli S, Batra RC. Derivation of plate and rod equations for a piezoelectric body from a mixed three-dimensional variational principle. J Elastic, in press.
[10] Robbins DH, Reddy JN. Analysis of piezoelectrically actuated beams using a layer-wise displacement theory. Comput Struct 1991;41:265–79.
[11] Heyliger P, Ramirez G, Saravanos D. Coupled discrete-layer finite elements for laminated piezoelectric plates. Commun Numer Meth Engng 1994;10:971–81.
[12] Batra RC, Liang XQ. Finite dynamic deformations of smart structures. Computat Mech 1997;20:427–38.
[13] Ray MC, Rao KM, Samanta B. Exact analysis of coupled electroelastic behavior of piezoelectric plate under cylindrical bending. Comput Struct 1992;45(4):667–77.
[14] Heyliger P, Brooks S. Exact solutions for laminated piezoelectric plates in cylindrical bending. J Appl Mech 1996;63:903–10.
[15] Yang JS, Batra RC, Liang XQ. The cylindrical bending vibration of a laminated elastic plate due to piezoelectric actuators. Smart Mater Struct 1994;3:485–93.
[16] Vel SS, Batra RC. Cylindrical bending of laminated plates with distributed and segmented piezoelectric actuators/sensors. AIAA J 2000;38:857–67.
[17] Vel SS, Batra RC. Three-dimensional analytical solution for hybrid multilayered piezo electric plates. J Appl Mech, 2000;67:558–67.
[18] Moulson AJ, Herbert JM. Electroceramics: materials, properties, applications. London: Chapman and Hall, 1990.
[19] Tzou HS. Development of a lightweight robot end-effector using polymeric piezoelectric bimorph. In: Proceedings of the 1989 IEEE International Conference on Robotics and Automation, vol. 14/19. Los Angeles: Computer Society, 1989. p. 1704–9.
[20] Jones RM. Mechanics of composite materials. Washington DC: Scripta Book Co, 1975.
[21] Benjeddou A, Trindade MA, Ohayon R. A unified beam finite element model for extension and shear piezoelectric actuation mechanisms. J Intell Mater Sys Struct 1997;8:1012–25.
[22] Tiersten HF. Linear piezoelectric plate vibrations. New York: Plenum Press, 1969.
[23] Wolfram S. The Mathematica book, 4th ed. New York: Cambridge University Press, 1999.
[24] Reissner E. The effect of transverse shear deformation on the bending of elastic plates. J Appl Mech 1945;12(2):69–77.
[25] Tang YY, Noor AK, Xu K. Assessment of computational models for thermoelectroelastic multilayered plates. Comput Struct 1996;61(5):915–33.
[26] Zhang XD, Sun CT. Formulation of an adaptive sandwich beam. Smart Mater Struct 1996;5:814–23.